

Full length article

On the photon counting error probability and its application in optical wireless communications

Konstantinos Yiannopoulos*, Nikos C. Sagias, Anthony C. Boucouvalas

Department of Informatics and Telecommunications, University of Peloponnese, Akadimaikou G.K. Vlachou, 22131 Tripoli, Greece



ARTICLE INFO

Article history:

Received 24 May 2018

Received in revised form 17 May 2019

Accepted 26 June 2019

Available online 2 July 2019

Keywords:

Error probability

Photon counting

Optical amplifiers

Optical wireless

Diversity reception

Negative-exponential fading

γ - γ fading

ABSTRACT

We present an efficient approach for the probability of error (PER) of photon counting statistics in a pre-amplified optical receiver. Our approach enables a fast and highly accurate calculation of the instantaneous PER, as well as the average PER in optical wireless communications. By utilizing the proposed approximation, we assess the performance of an equal gain combiner (EGC) and a selection combiner (SC) in negative-exponential and γ - γ fading. The results show that the EGC provides a significant link gain under all fading conditions, while the SC is only viable in strong turbulence.

© 2019 Elsevier B.V. All rights reserved.

1. Introduction

Optical amplification has been extensively studied in optical wireless communications (OWC) for the compensation of the signal fades that are introduced when optical beams propagate through turbulent media [1], such as the atmosphere or the sea. Amplifiers have been considered in diversity reception [2–4], relaying [5–7] and signal regeneration [8–10], with a goal to improve the received signal quality, and therefore, the PER in the presence of fading.

The PER of the optical receiver is strongly affected but the noise that is added to the signal during amplification. In direct detection, the received signal beats with the amplifier noise and is either modeled as a continuous Gaussian/chi-squared random variable (RV) [11,12], or as a discrete photon count that follows a Laguerre probability mass function (pmf) [13]. In the latter description, the detected photon count amounts to several hundreds or thousands for typical amplifier gains and the calculation of the PER proves time consuming, since extensive summations that involve the Laguerre distribution are required. Furthermore, the calculation of the average PER proves even more challenging in an OWC system, given that the PER must be calculated for all possible channel states.

In this work, we present an efficient approach for calculating the PER in pre-amplified systems that are modeled using Laguerre statistics. Our approach is derived from the integral form of the

Laguerre polynomials and limits the number of terms that are required to calculate the PER from several hundreds/thousands to a couple of tens, thus significantly reducing the PER calculation time. Moreover, we demonstrate that it remains equally accurate for a range of amplifier gains and optical signal-to-noise ratios (OSNRs) without imposing significant calculation overheads. Given the limited number of terms that are required, the approximation is well suited for the calculation of the average PER in OWCs, either analytically or numerically. We perform the assessment of the average PER of the pre-amplified receiver in strong, moderate and weak turbulence conditions. In addition, we provide analytical and numerical results for receivers with EGC and SC diversity reception. Our results show that the EGC is suitable for all turbulence conditions, which is in close agreement with a recent work where we demonstrate that the EGC is “almost optimal” in pre-amplified systems [14]. The SC performs worse than the EGC in all cases, and also performs worse than a single receiver system in weak turbulence.

The rest of this paper is structured as follows: In Section 2 we present the novel PER approach and compare it with the standard one. Section 3 details the OWC system with diversity and provides instantaneous PER expressions for EGC and SC. Finally, Sections 4 and 5 present the average PER performance of the two combiners in negative exponential (strong) and γ - γ (moderate/weak) turbulence, respectively. The two fading distributions are in good agreement with channel measurements and simulations in OWC systems [1,15,16], but do not limit the applicability of the presented method. The method can be readily extended in more generalized fading distributions [16,17], as well

* Corresponding author.

E-mail address: kyianno@uop.gr (K. Yiannopoulos).

as distributions that model both fading and pointing-errors [18–21].

2. Photon counter PER

The system under consideration consists of a laser modulating the information bit stream using on-off keying (OOK) and an optically pre-amplified receiver [2]. At the receiving side, an optical antenna, i.e. an aperture with adequately large field-of-view, collects the incoming light and feeds it to the amplifier. The amplifier boosts the signal intensity and also adds amplified spontaneous emission (ASE) noise. An optical filter is utilized to reject out-of-band noise and a polarizer discards any noise that is not co-polarized with the signal. The filtered optical signal is then fed to the photon-counter, which can be implemented by a photodiode and a time-domain integrator [22]. We assume that the photon counter is ideal and that it produces a discrete photon count n per bit.

Due to the amplified spontaneous noise from the amplifier, the photon count corresponds to a Laguerre RV with pmf [22]

$$p(n, \mu_s, M) = \frac{\lambda^n \exp\left(-\frac{\mu_s}{1+\lambda}\right)}{(1+\lambda)^{n+M}} L_n^{M-1}\left[-\frac{\mu_s}{\lambda(1+\lambda)}\right], \quad (1)$$

where $\lambda = \mu_n/M$, μ_s and $\mu_n = n_{sp}(G-1)M$ denote the average number of amplified signal and noise photons, respectively, G is the amplifier gain, n_{sp} is the amplifier population inversion factor, M equals the number of modes (approximately equal to the product of the optical filter bandwidth and the bit duration), and $L_n^{M-1}(\cdot)$ stands for the associated Laguerre polynomial [23, eq. (8.970/1)].

2.1. Standard PER analytical approach

In OOK the receiver examines the photon count n and decides on the reception of bits '1' and '0' by comparing with a threshold n_{th} . Assuming an equal probability of occurrence for both bits, the PER is given by

$$P_e(n_{th}, \mu_s, M) = \frac{P_0(n_{th}, M) + P_1(n_{th}, \mu_s, M)}{2}, \quad (2)$$

where

$$P_0(n_{th}, M) = \sum_{k=n_{th}+1}^{\infty} p(k, 0, M) \quad (3)$$

and

$$P_1(n_{th}, \mu_s, M) = \sum_{k=0}^{n_{th}} p(k, \mu_s, M), \quad (4)$$

while the optimal decision threshold n_{th}^* , that minimizes P_e , is calculated in a log-likelihood fashion as

$$p(n_{th}^*, 0, M) = p(n_{th}^*, \mu_s, M). \quad (5)$$

Note that (3) is in the form of an infinite series representation. Also (4) includes a finite sum of Laguerre polynomials where a large number of terms must be summed. Thus, (3) and (4) cannot be directly used for the numerical evaluation of the error probability in (2), while alternative simplified expressions are not available to our knowledge.

2.2. Computationally efficient PER analytical approach

Using (3), we evaluate an analytical expression for the error probability in '0' bits. For convenience we here first define $y =$

$\lambda/(1+\lambda)$, and calculate

$$\begin{aligned} P_0(n_{th}, M) &= (1-y)^M \sum_{k=n_{th}+1}^{\infty} \binom{k+M-1}{k} y^k \\ &= 1 - (1-y)^M \sum_{k=0}^{n_{th}} \binom{k+M-1}{k} y^k \\ &= \frac{B_y(n_{th}+1, M)}{B(n_{th}+1, M)} \\ &= \frac{(n_{th}+M)!}{(n_{th}+1)!(M-1)!} y^{n_{th}+1} {}_2F_1(n_{th}+1, 1-M; n_{th}+2; y), \end{aligned} \quad (6a)$$

with $\binom{a}{b}$ denoting the binomial co-efficient, $B_y(\cdot, \cdot)$ being the incomplete beta function [23, eq. (8.391)] and ${}_2F_1(\cdot, \cdot; \cdot; \cdot)$ being the Gauss hypergeometric function [23, eq. (9.100)]. We further apply transform [23, eq. (9.131.1)] to evaluate P_0 as

$$\begin{aligned} P_0(n_{th}, M) &= \frac{\lambda^{n_{th}+1}}{(1+\lambda)^{n_{th}+M+1}} \binom{n_{th}+M}{n_{th}+1} \\ &\quad \times {}_2F_1\left(1, n_{th}+M+1; n_{th}+2; \frac{\lambda}{1+\lambda}\right). \end{aligned} \quad (6b)$$

In order to derive a simple to evaluate expression for P_1 we use an integral representation of Laguerre polynomials

$$L_k^{M-1}(t) = \frac{1}{2\pi j} \oint_C \frac{\exp\left(-\frac{zt}{1-z}\right)}{(1-z)^M z^{k+1}} dz, \quad (7)$$

where $j = \sqrt{-1}$ and C is a contour of integration that encloses the origin, but not the singularity at $z = 1$. We here define $t = -\mu_s/[\lambda(1+\lambda)]$ and calculate $I = \sum_{k=0}^{n_{th}} y^k L_k^{M-1}(t)$ with the help of (7) as

$$\begin{aligned} I &= \frac{1}{2\pi j} \oint_C \frac{\exp\left(-\frac{zt}{1-z}\right)}{(1-z)^M z} \sum_{k=0}^{n_{th}} \left(\frac{y}{z}\right)^k dz \\ &= \frac{1}{2\pi j} \oint_C \frac{\exp\left(-\frac{zt}{1-z}\right)}{(1-z)^M z} \frac{\left(\frac{y}{z}\right)^{n_{th}+1} - 1}{\left(\frac{y}{z}\right) - 1} dz \\ &= \frac{y^{n_{th}+1}}{2\pi j} \oint_C \frac{\exp\left(-\frac{zt}{1-z}\right)}{(1-z)^M z^{n_{th}+1} (y-z)} dz \\ &\quad - \frac{1}{2\pi j} \oint_C \frac{\exp\left(-\frac{zt}{1-z}\right)}{(1-z)^M (y-z)} dz. \end{aligned} \quad (8)$$

After noting that $y < 1$ in a pre-amplified system, it is straightforward to verify that the second integral equals zero, since the integrand has no poles within C . Moreover, the first integral can be re-written as

$$\begin{aligned} I &= \frac{y^{n_{th}+1}}{2\pi j} \oint_C \frac{\exp\left(-\frac{zt}{1-z}\right) z^{-(n_{th}+1)}}{(1-z)^{M+1} \left[1 - \frac{(\lambda+1)^{-1}}{1-z}\right]} dz \\ &= \frac{y^{n_{th}+1}}{2\pi j} \oint_C \frac{\exp\left(-\frac{zt}{1-z}\right)}{(1-z)^{M+1} z^{n_{th}+1}} \sum_{k=0}^{\infty} \frac{(\lambda+1)^{-k}}{(1-z)^k} dz \\ &= \frac{y^{n_{th}+1}}{2\pi j} \sum_{k=0}^{\infty} \frac{1}{(\lambda+1)^k} \oint_C \frac{\exp\left(-\frac{zt}{1-z}\right) z^{-(n_{th}+1)}}{(1-z)^{M+1+k}} dz \\ &= y^{n_{th}+1} \sum_{k=0}^{\infty} \frac{1}{(\lambda+1)^k} L_n^{M+k}(t). \end{aligned} \quad (9)$$

Table 1
Number of terms required for a relative error of 10^{-3} .

	$G = 10$	$G = 100$	$G = 1000$
n_{th}	125	1371	13830
n_0	12	11	15

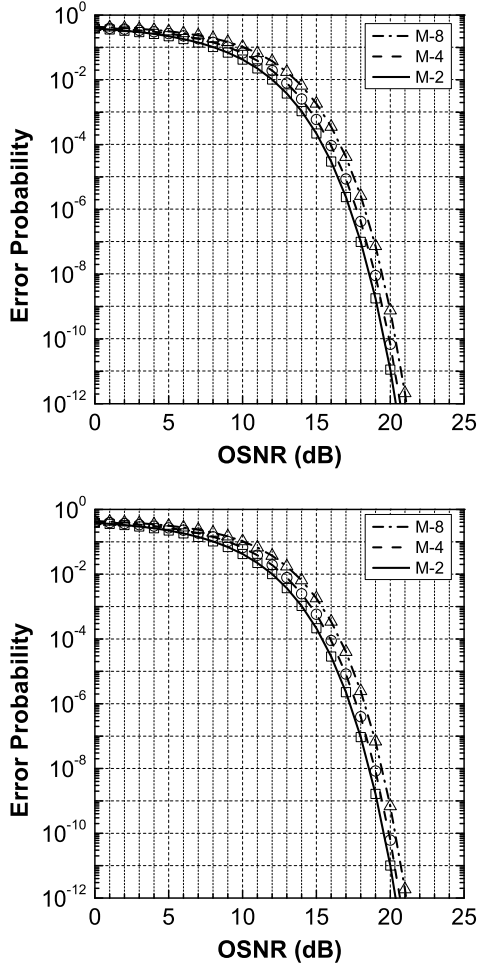


Fig. 1. Error probability for a $G = 100$ (top) and $G = 1000$ (bottom) amplifier. The solid plots correspond to the exact calculation and the plot points correspond to the proposed approximation. $n_0 = 20$ terms are used for the PER approximation.

Finally, after combining (1), (4) and (9), we find that

$$P_1(n_{th}, \mu_s, M) = \left(\frac{\lambda}{1+\lambda}\right)^{n_{th}+1} \exp\left(-\frac{\mu_s}{1+\lambda}\right) \times \sum_{k=M}^{\infty} \frac{1}{(1+\lambda)^k} L_{n_{th}}^k\left[-\frac{\mu_s}{\lambda(1+\lambda)}\right]. \quad (10)$$

By comparing (10) with (4), we observe that (10) includes an infinite sum of Laguerre polynomials. However, since in pre-amplified systems $\lambda \gg 1$, the series in (10) is converging fast. In contrast, the numerical evaluation of (4) imposes that all $n_{th} + 1 \gg 1$ terms must be used. Therefore, (10) is practically much simpler to numerically evaluate P_1 . In Table 1 we compare the number of terms n_0 that are required to evaluate P_1 using (10) as well as (4), with a relative error of 0.1% for an OSNR = $\mu_s/\lambda = 15$ dB, $n_{sp} = 1$ and $M = 4$. From this table it can be easily concluded that only a few terms are sufficient for (10) to achieve the target relative error for any value of G . More accurate results can be

also obtained by including additional terms with the help of the following recursive relations for the Laguerre polynomials

$$L_{n-1}^{k+1}(t) = \frac{n+k}{t} L_{n-1}^k(t) - \frac{n}{t} L_n^k(t), \quad (11a)$$

and

$$L_n^{k+1}(t) = L_{n-1}^{k+1}(t) + L_n^k(t). \quad (11b)$$

Since the above expressions introduce minimal overhead, the computational time of (10) is mainly determined by the calculation time of $L_{n_{th}-1}^M(t)$ and $L_{n_{th}}^M(t)$. Both can be calculated relatively fast and accurately using standard mathematical software packages.

The error probability (both using (4) and (10)) is plotted in Fig. 1 against the OSNR for an amplifier with gain $G = 100$ and $n_{sp} = 1$. The first $n_0 = 20$ terms are kept for the approximation and the figure shows that the exact and approximated results coincide. In fact, the approximation has been tested to provide the exact results for OSNRs up to 30 dB that correspond to unrealistically low error probabilities and are not included in the figure. On the other hand, the inclusion of so few terms means that the calculation time of the error probability is drastically reduced. In standard computer hardware and mathematical packages, the approximate calculation takes less than 1 s to complete irrespective of the OSNR, while the exact calculation may last for several secs or tens of secs. When the amplifier gain is increased to $G = 1000$, our approximation remains equally accurate and computationally efficient, despite the fact that the signal and noise photon counts are increased by a factor of 10. The corresponding PER results are also shown in Fig. 1, where the same number of summation terms ($n_0 = 20$) have been utilized in the approximation. Given that the increase on the amplifier gain does not impact the computational efficiency and that the PER performance of both amplifiers is practically identical, we only consider the $G = 100$ case for application in OWC systems. The utilization of higher gain amplifiers is not expected to significantly alter the system performance.

3. OWC system model and average PER

We now consider the performance of the pre-amplified detector in an OWC system, where the number of received signal photons μ_s is affected by the turbulent nature of the atmosphere. We assume that the bit period is much smaller than the fading timescales (typically msec), therefore the atmospheric channel state does not change within a counting interval. The average number of photons that are received μ_s also remains constant within this interval and the previously presented PER expressions remain valid for each individual photon count. However, μ_s also closely follows the stochastic channel response over longer timescales and it can be treated as a RV that follows the fading distribution [2,24,25], producing lower photon counts and higher PERs when the channel is in a fade.

The impact of the turbulence is partially mitigated by introducing L identical reception branches, as shown in Fig. 2. Adequate lateral separation between the optical antennas is also considered to ensure that the received signals are statistically independent. Each branch produces an instantaneous photon count n_ℓ , $\ell = 1, 2, \dots, L$ following a Laguerre pmf, with shape determined by $\mu_{s,\ell}$ signal photons received in the ℓ th branch. The photon counts are then linearly combined and the detector decides upon the bit reception.

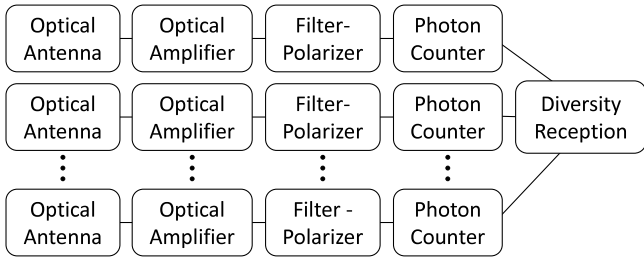


Fig. 2. Multibranch OWC system model.

3.1. EGC and SC average PER

In this work we focus on two linear combiners: the EGC, which adds the photon counts from all branches, and the SC, which only considers the photon count in the branch with the highest instantaneous optical signal power. For identical reception branches, the pmf of the instantaneous EGC photon count $n = \sum_{\ell=1}^L n_{\ell}$ is obtained by L successive convolutions of (1). Given the addition formula for Laguerre polynomials [23, eq. (8.974/4)], the convolution results in [2]

$$p_{egc}(n, \mu_s, L, M) = p(n, \mu_s, LM), \quad (12)$$

where $\mu_s = \sum_{\ell=1}^L \mu_{s,\ell}$ equals the sum of signal photons that are received in all branches. Given μ_s , the instantaneous PER of EGC is then calculated from (2) as

$$P_{e, egc}(n_{th}, \mu_s, L, M) = P_e(n_{th}, \mu_s, LM). \quad (13)$$

Moreover, for SC the instantaneous PER is calculated from (2) as

$$P_{e, sc}(n_{th}, \mu_s, L, M) = P_e(n_{th}, \mu_s, M), \quad (14)$$

with $\mu_s = \max\{\mu_{s,\ell}\}$, since only one branch is selected.

The average PER of EGC and SC can be obtained by integrating (13) and (14), respectively, over all possible states of the photon count μ_s , i.e.

$$\bar{P}_e = \int_x P_e(n_{th}, x, L, M) f_{\mu_s}(x) dx, \quad (15)$$

where $f_{\mu_s}(\cdot)$ denotes the probability density function (pdf) of μ_s .

3.2. Optimal decision threshold

The decision threshold n_{th} plays an important role in evaluating the average PER in (15), based on which, two receiver types can be implemented. If the instantaneous channel-state information (CSI) is available at the receiver, then n_{th} is constantly adapted to the optimal value for the corresponding channel state x following

$$p(n_{th}^*, x, LM) = p(n_{th}^*, 0, LM), \quad (16a)$$

and

$$p(n_{th}^*, x, M) = p(n_{th}^*, 0, M), \quad (16b)$$

for EGC and SC, respectively. If CSI is not available, then a fixed optimal threshold is utilized. In the results that are presented in the following sections for non-CSI receivers, we evaluate the optimal threshold by minimizing (15) numerically. The minimization process requires the calculation of (15) for a limited number of thresholds [26], and each calculation is performed in an efficient manner using the proposed approach.

4. Average PER over negative exponential fading

4.1. Equal gain combiner

The calculation of the average PER requires the knowledge of the fading distribution of $\mu_s = \sum_{\ell=1}^L \mu_{s,\ell}$, where each $\mu_{s,\ell}$ follows a NE pdf

$$f_{\mu_{s,\ell}}(x) = \frac{L}{\mu_s} \exp\left(-\frac{Lx}{\mu_s}\right), \quad (17)$$

with $\bar{\mu}_s$ corresponding to the total average number of photons that arrive at the combiner input. Given that the sum of iid NE RVs follows an Erlang distribution, the pdf of μ_s is

$$f_{\mu_s}(x) = \left(\frac{L}{\bar{\mu}_s}\right)^L \frac{x^{L-1}}{(L-1)!} \exp\left(-\frac{Lx}{\bar{\mu}_s}\right). \quad (18)$$

Using (13), (15) and (18) and

$$\begin{aligned} \int_0^\infty \frac{x^{L-1}}{(L-1)!} L^n(-bx) \exp(-cx) dx &= \\ &= \sum_{j=0}^n \binom{n+a}{n-j} \frac{(j+L-1)!}{j!(L-1)!} b^j c^{-j-L} = \\ &= \binom{n+a}{n} c^{-L} {}_2F_1\left(L, -n; a+1; -\frac{b}{c}\right), \end{aligned} \quad (19)$$

with $a = LM + i$, $b = 1/[\lambda(1+\lambda)]$, $c = (1+\lambda + \bar{\mu}_s/L)/[(1+\lambda)\bar{\mu}_s/L]$, the average PER of a non-CSI receiver can be analytically evaluated as

$$\bar{P}_{e, egc} = \frac{1}{2} (\bar{P}_{1, egc} + \bar{P}_{0, egc}), \quad (20)$$

with

$$\begin{aligned} \bar{P}_{1, egc} &= \left(\frac{1+\lambda}{1+\lambda + \bar{\mu}_s/L}\right)^L \left(\frac{\lambda}{1+\lambda}\right)^{n_{th}+1} \\ &\times \sum_{i=L}^\infty \binom{n_{th}+i}{n_{th}} \frac{1}{(1+\lambda)^i} \\ &\times {}_2F_1\left[L, -n_{th}; i+1; -\frac{\bar{\mu}_s/L}{\lambda(1+\lambda + \bar{\mu}_s/L)}\right] \end{aligned} \quad (21)$$

and

$$\bar{P}_{0, egc} = P_0(n_{th}, LM). \quad (22)$$

If a CSI receiver is utilized, then (15) can be evaluated by numerical integration with the help of (13), (16a) and (18).

4.2. Selection combiner

In NE exponential fading, the SC signal photon count μ_s is distributed as

$$\begin{aligned} f_{\mu_s}(x) &= L \left(\int_0^x f_{\mu_{s,\ell}}(\tau) d\tau \right)^{L-1} f_{\mu_{s,\ell}}(x) \\ &= \frac{L^2}{\bar{\mu}_s} \exp\left(-\frac{Lx}{\bar{\mu}_s}\right) \left[1 - \exp\left(-\frac{Lx}{\bar{\mu}_s}\right) \right]^{L-1} \\ &= \frac{L^2}{\bar{\mu}_s} \sum_{\ell=0}^{L-1} \binom{L-1}{\ell} (-1)^\ell \exp\left[-\frac{L(\ell+1)x}{\bar{\mu}_s}\right]. \end{aligned} \quad (23)$$

The average PER of a non-CSI receiver can be analytically calculated from (2), (15) and (23) using (19), yielding

$$\bar{P}_{e, sc} = \frac{1}{2} (\bar{P}_{1, sc} + \bar{P}_{0, sc}), \quad (24)$$

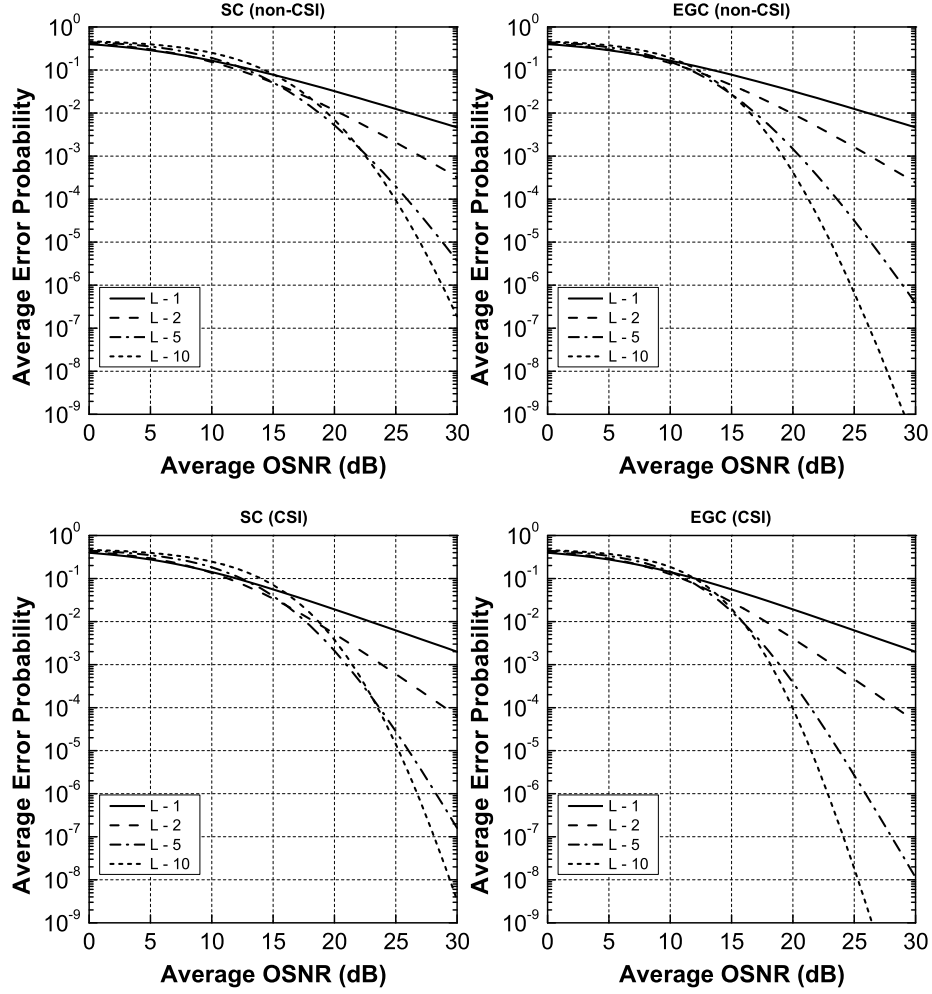


Fig. 3. Average error probability for a $G = 100$ amplifier and $M = 2$ modes for non-CSI (top) and CSI (bottom) receivers in negative exponential fading. $n_0 = 20$ terms are used for the PER approximation.

with

$$\begin{aligned} \bar{P}_{1,sc} &= \left(\frac{\lambda}{1+\lambda} \right)^{n_{th}+1} \sum_{\ell=0}^{L-1} \sum_{i=M}^{\infty} \binom{L-1}{\ell} (-1)^\ell \\ &\times \frac{(1+\lambda)L}{(1+\lambda)(\ell+1) + \bar{\mu}_s/L} \binom{n_{th}+i}{n_{th}} \left(\frac{1}{1+\lambda} \right)^i \\ &\times {}_2F_1 \left\{ 1, -n_{th}; i+1; -\frac{\bar{\mu}_s/L}{\lambda[(1+\lambda)(\ell+1) + \bar{\mu}_s/L]} \right\} \end{aligned} \quad (25)$$

and

$$\bar{P}_{0,sc} = P_0(n_{th}, M). \quad (26)$$

Moreover, a CSI receiver requires the numerical evaluation of (15) using the instantaneous PER from (14), the adaptive threshold from (16b) and the fading statistics from (23).

4.3. Results and discussion

Fig. 3 illustrates the average error probability of the EGC and the SC (both non-CSI and CSI) against the average OSNR $\bar{\mu}_s/\lambda$ for a $G = 100$ amplifier. Diversity orders of $L = 1 - 10$ are considered, so as to demonstrate the efficiency of the presented approximation. By comparing the two figures, it becomes evident that the CSI awareness provides a gain of approximately 1–3 dB for both combiners. Moreover, the two combiners perform closely for low diversity orders, but the EGC significantly outperforms the

SC as more branches are introduced in the system. For $L = 5$ the non-CSI EGC performs slightly worse than the CSI SC, while for $L = 10$ the non-CSI EGC is actually better than the CSI SC. These results are in close agreement with previous works, where it has been demonstrated that the EGC is an “almost-optimal” combiner in pre-amplified OWC systems [14]. Finally, it is possible to identify scenarios that allow for trade-offs between cost (number of branches) and receiver/combiner complexity (channel and signal power estimation). Considering for example an average PER between 10^{-3} to 10^{-4} , one may achieve similar performance by utilizing a non-CSI EGC with $L = 10$ or a CSI EGC with $L = 5$. Equivalent performance is also observed for aforementioned PERs between the $L = 5$ non-CSI EGC and the $L = 5$ CSI SC.

5. Average PER over $\gamma - \gamma$ fading

In $\gamma - \gamma$ fading, each received signal is distributed according to the following pdf

$$\begin{aligned} f_{\mu_s, \ell}(x) &= \frac{2 (m_y m_x)^{\frac{m_y+m_x}{2}}}{\Gamma(m_x) \Gamma(m_y)} x^{\frac{m_y+m_x}{2}} \left(\frac{Lx}{\bar{\mu}_s} \right)^{\frac{m_y+m_x}{2}} \\ &\times K_{m_y-m_x} \left(2 \sqrt{m_y m_x \frac{Lx}{\bar{\mu}_s}} \right), \end{aligned} \quad (27)$$

where m_x and m_y are related to the effective numbers of large- and small-scale scatterers in the OWC link and $\Gamma(\cdot)$ and $K_v(\cdot)$

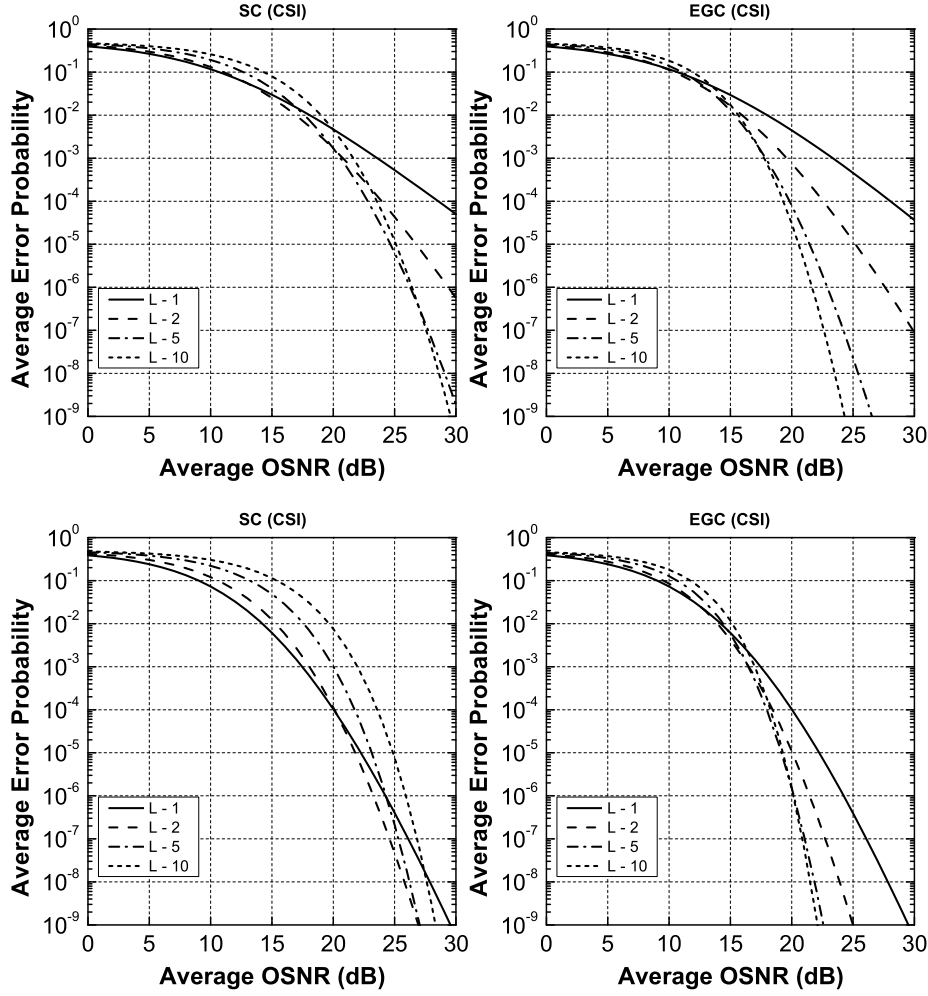


Fig. 4. Average error probability for a $G = 100$ amplifier and $M = 2$ modes in moderate (top) and weak (bottom) $\gamma - \gamma$ fading. $n_0 = 20$ terms are used for the PER approximation.

denote the Gamma and second-kind modified Bessel functions, respectively. Assuming a plane wave transmission [1], we utilize the following formulas to calculate parameters m_x and m_y

$$m_x = \frac{1}{\exp(\sigma_{\ln x}^2) - 1}, \quad (28)$$

$$m_y = \frac{1}{\exp(\sigma_{\ln y}^2) - 1},$$

respectively. The log-intensity variances are given by

$$\sigma_{\ln x}^2 = \frac{0.49 \sigma_R^2}{(1 + 1.11 \sigma_R^{12/5})^{7/6}}, \quad (29)$$

$$\sigma_{\ln y}^2 = \frac{0.51 \sigma_R^2}{(1 + 0.69 \sigma_R^{12/5})^{5/6}},$$

and the Rytov variance equals

$$\sigma_R^2 = 1.23 C_n^2 k^{7/6} l^{11/6}, \quad (30)$$

where l is the link length, k is the wavenumber and C_n^2 is the refractive index structure parameter. Table 2 summarizes the m_x and m_y values that have been obtained for a link that operates at 1550 nm and a structure constant of $C_n^2 = 4.58 \cdot 10^{-13} \text{ m}^{-2/3}$.

The EGC fading statistics require knowledge of the distribution of the sum of iid $\gamma - \gamma$ RVs following (12), which is not known

Table 2
 $\gamma - \gamma$ parameters.

l (m)	σ_R^2	m_x	m_y
155	0.3	8.43	6.92
345	1.3	4.13	2.16

Table 3
 $\alpha - \mu$ parameters.

	$l = 155 \text{ m}$			$l = 345 \text{ m}$		
	$L - 2$	$L - 5$	$L - 10$	$L - 2$	$L - 5$	$L - 10$
α	0.48	0.46	0.45	0.48	0.43	0.41
μ	32.05	86.41	177.81	11.19	33.51	72.93
$\hat{\chi}$	1.93	4.93	9.92	1.82	4.78	9.77

and has to be approximated. An accurate approximation results from fitting the four first $\gamma - \gamma$ moments to an $\alpha - \mu$ distribution [27]

$$f_{\mu_s}(x) = \frac{\alpha \mu^\mu x^{\alpha\mu-1}}{\hat{\chi}^{\alpha\mu} \Gamma(\mu)} \exp\left(-\mu \frac{x^\alpha}{\hat{\chi}^\alpha}\right). \quad (31)$$

The calculation of parameters α , μ and $\hat{\chi}$ is described in detail in [28], and Table 3 summarizes their values for the link and diversity arrangements under consideration. The SC fading

statistics are evaluated directly from

$$f_{\mu_s}(x) = L \left(\int_0^x f_{\mu_s, \ell}(\tau) d\tau \right)^{L-1} f_{\mu_s, \ell}(x). \quad (32)$$

Even though both CSI and non-CSI receivers can be studied in $\gamma - \gamma$ fading, we focus on the former since they exhibit superior performance. Fig. 4 summarizes the average PER of a CSI receiver for the medium ($m_x = 4.13$, $m_y = 2.16$) and weak ($m_x = 8.43$, $m_y = 6.92$) turbulence link. Similar to the NE scenario, the EGC provides a significant performance enhancement which also becomes better with the number of the receiving branches in moderate fading. The SC performance initially improves, but an increase in the number of branches from five to ten does not impart a considerable improvement; in fact the $L = 5$ combiner performs better for an average PER greater than 10^{-7} . With respect to weak fading, the SC is performing even worse and a $L = 5$, 10 branch combiner actually introduces a degradation when compared to a single receiver system. This is to be expected, since the SC disregards branches with a potentially high OSNR in weak fading. The EGC generally benefits from additional branches in weak fading, but there is only but a small gain from increasing the number of branches over $L = 5$.

6. Conclusion

We have presented an approximation for the PER in pre-amplified optical receivers in photon counting statistics. The approximation reduces the number of terms that are required for the PER calculation and remains equally efficient for typical amplifier gains irrespective of the OSNR. We have also utilized the approximation to provide analytical and numerical results on the average PER of pre-amplified diversity reception that employs an EGC or a SC in weak, moderate and strong fading. Given its efficiency, the approximation can be utilized to assess the performance of other fading statistics, combiners and/or higher order modulation formats via analytical, numerical or simulation methods.

Declaration of competing interest

No author associated with this paper has disclosed any potential or pertinent conflicts which may be perceived to have impending conflict with this work. For full disclosure statements refer to <https://doi.org/10.1016/j.phycom.2019.100756>.

References

- [1] L.C. Andrews, R.L. Phillips, *Laser Beam Propagation Through Random Media*, second ed., SPIE Press, Bellingham, Washington, 2005.
- [2] M. Razavi, J.H. Shapiro, Wireless optical communications via diversity reception and optical preamplification, 4 (3) 2005 975–983. <http://dx.doi.org/10.1109/TWC.2005.847102>.
- [3] A.O. Aladeloba, A.J. Phillips, M.S. Woolfson, Improved bit error rate evaluation for optically pre-amplified free-space optical communication systems in turbulent atmosphere, IET Optoelectron. (ISSN: 1751-8768) 6 (1) (2012) 26–33, <http://dx.doi.org/10.1080/09500340.2013.831137>.
- [4] W. Zhao, Y. Han, X. Yi, Error performance analysis for fso systems with diversity reception and optical preamplification over gamma-gamma atmospheric turbulence channels, J. Modern Opt. 60 (13) (2013) 1060–1068, <http://dx.doi.org/10.1080/09500340.2013.831137>.
- [5] S. Kazemlou, S. Hranilovic, S. Kumar, All-optical multihop free-space optical communication systems, J. Lightwave Technol. (ISSN: 0733-8724) 29 (18) (2011) 2663–2669, <http://dx.doi.org/10.1109/JLT.2011.2160615>.
- [6] E. Bayaki, D.S. Michalopoulos, R. Schober, EDFA-based all-optical relaying in free-space optical systems, (ISSN: 0090-6778) 60 (12) (2012) 3797–3807, <http://dx.doi.org/10.1109/TCOMM.2012.090512.110198>.
- [7] M.A. Kashani, M.M. Rad, M. Safari, M. Uysal, All-optical amplify-and-forward relaying system for atmospheric channels, IEEE Commun. Lett. (ISSN: 1089-7798) 16 (10) (2012) 1684–1687, <http://dx.doi.org/10.1109/LCOMM.2012.082012.121066>.
- [8] M. Abtahi, P. Lemieux, W. Mathlouthi, L.A. Rusch, Suppression of Turbulence-Induced Scintillation in Free-Space Optical Communication Systems Using Saturated Optical Amplifiers, 24 (12) 2006 4966–4973. <http://dx.doi.org/10.1109/JLT.2006.884561>.
- [9] K. Yiannopoulos, N.C. Sagias, A.C. Boucouvalas, Fade Mitigation Based on Semiconductor Optical Amplifiers, 31 (23) 2013 3621–3630. <http://dx.doi.org/10.1109/JLT.2013.2285260>.
- [10] P.V. Trinh, N.T. Dang, A.T. Pham, All-optical relaying fso systems using edfa combined with optical hard-limiter over atmospheric turbulence channels, J. Lightwave Technol. 33 (19) (2015) 4132–4144, <http://dx.doi.org/10.1109/JLT.2015.2466432>.
- [11] N.A. Olsson, Lightwave systems with optical amplifiers, 7 (7) 1989 1071–1082. <http://dx.doi.org/10.1109/50.29634>.
- [12] P.A. Humblet, M. Azizoglu, On the bit error rate of lightwave systems with optical amplifiers, 9 (11) 1991 1576–1582. <http://dx.doi.org/10.1109/50.97649>.
- [13] S.K. Robert M. Gagliardi, *Optical Communications*, first ed., Wiley, 1976.
- [14] K. Yiannopoulos, N.C. Sagias, A.C. Boucouvalas, K. Peppas, Optimal combining for optical wireless systems with amplification: the χ^2 noise regime, IEEE Photonics Technol. Lett. (ISSN: 1041-1135) 30 (1) (2018) 119–122, <http://dx.doi.org/10.1109/LPT.2017.2777908>.
- [15] F.S. Vetelino, C. Young, L. Andrews, J. Recolons, Aperture averaging effects on the probability density of irradiance fluctuations in moderate-to-strong turbulence, Appl. Opt. 46 (11) (2007) 2099–2108, <http://dx.doi.org/10.1364/AO.46.002099>.
- [16] A. Jurado-Navas, J.M. Garrido-Balsells, J.F. Paris, A. Puerta-Notario, A unifying statistical model for atmospheric optical scintillation, in: J. Awrejcewicz (Ed.), Numerical Simulations of Physical and Engineering Processes, IntechOpen, Rijeka, 2011, <http://dx.doi.org/10.5772/25097>.
- [17] N. Joshi, P.K. Sharma, Performance of wireless optical communication in S -distributed turbulence, IEEE Photonics Technol. Lett. (ISSN: 1041-1135) 28 (2) (2016) 151–154, <http://dx.doi.org/10.1109/LPT.2015.2487605>.
- [18] A.A. Farid, S. Hranilovic, Outage capacity optimization for free-space optical links with pointing errors, J. Lightwave Technol. (ISSN: 0733-8724) 25 (7) (2007) 1702–1710, <http://dx.doi.org/10.1109/JLT.2007.899174>.
- [19] I.S. Ansari, F. Yilmaz, M. Alouini, Performance Analysis of Free-Space Optical Links Over Málaga (\mathcal{M}) Turbulence Channels With Pointing Errors, IEEE Trans. Wirel. Commun. (ISSN: 1536-1276) 15 (1) (2016) 91–102, <http://dx.doi.org/10.1109/TWC.2015.2467386>.
- [20] P.K. Sharma, A. Bansal, P. Garg, Relay assisted bi-directional communication in generalized turbulence fading, J. Lightwave Technol. (ISSN: 0733-8724) 33 (1) (2015) 133–139, <http://dx.doi.org/10.1109/JLT.2014.2379950>.
- [21] N.I. Miridakis, T.A. Tsiftsis, Egc reception for fso systems under mixture-gamma fading channels and pointing errors, IEEE Commun. Lett. (ISSN: 1089-7798) 21 (6) (2017) 1441–1444, <http://dx.doi.org/10.1109/LCOMM.2017.2670565>.
- [22] P. Martelli, S.M. Pietralunga, D. Nicodemi, M. Martinelli, Accurate sensitivity in optically preamplified direct detection, Opt. Lett. 29 (13) (2004) 1473–1475, <http://dx.doi.org/10.1364/OL.29.001473>.
- [23] I.S. Gradshteyn, I.M. Ryzhik, Table of integrals, series, and products, 7, Elsevier/Academic Press, Amsterdam, 2007, xlviii+1171.
- [24] M.C. Teich, S. Rosenberg, Photocounting array receivers for optical communication through the lognormal atmospheric channel. 1: Optimum and suboptimum receiver structures, Appl. Opt. 12 (11) (1973) 2616–2624, <http://dx.doi.org/10.1364/AO.12.002616>, <http://ao.osa.org/abstract.cfm?URI=ao-12-11-2616>.
- [25] S.G. Wilson, M. Brandt-Pearce, Qianling Cao, J.H. Leveque, Free-space optical mimo transmission with q-ary ppm, IEEE Trans. Commun. (ISSN: 0090-6778) 53 (8) (2005) 1402–1412, <http://dx.doi.org/10.1109/TCOMM.2005.852836>.
- [26] R. Brent, *Algorithms for minimization without derivatives*, Prentice-Hall, ISBN: 0-13-022335-2, 1973.
- [27] M.D. Yacoub, The $\alpha - \mu$ distribution: A physical fading model for the stacy distribution, IEEE Trans. Veh. Technol. (ISSN: 0018-9545) 56 (1) (2007) 27–34, <http://dx.doi.org/10.1109/TVT.2006.883753>.
- [28] K.P. Peppas, A simple, accurate approximation to the sum of gamma-gamma variates and applications in mimo free-space optical systems, IEEE Photonics Technol. Lett. (ISSN: 1041-1135) 23 (13) (2011) 839–841, <http://dx.doi.org/10.1109/LPT.2011.2135342>.



Konstantinos Yiannopoulos received the Diploma and Ph.D. in Electrical and Computer Engineering at 2000 and 2004, respectively, from the School of Electrical and Computer Engineering of the National Technical University of Athens, Greece.

Dr. Yiannopoulos is an Assistant Professor at the University of Peloponnese, Greece. He was a member of the research teams of the Photonics Communications Research Laboratory at the National Technical University of Athens, Greece, from 2000 to 2004, and the Computer Networks Laboratory at the University of

Patras, Greece, from 2005 to 2010. During this period, he conducted research on physical layer (optical signal processing, ultrafast optical sources, all-optical logic) and network layer (optical packet and burst switching networks) aspects of optical networks. At the present time, he is conducting research that focuses on optical wireless networks (system architectures and protocol analysis).

Dr. Yiannopoulos has more than 70 published papers in international journals and conferences. His research work was granted with the "IEEE/LEOS Graduate Student Fellowship Program 2004" award and has received more than 900 citations.



Nikos C. Sagias was born in Athens, Greece in 1974. He received the B.Sc. degree from the department of Physics (DoP) of the University of Athens (UoA), Greece in 1998. The M.Sc. and Ph.D. degrees in Telecommunication Engineering were received both from the UoA in 2000 and 2005, respectively. Since 2001, he has been involved in various National and European Research & Development projects for the Institute of Space Applications and Remote Sensing of the National Observatory of Athens, Greece. During 2006–2008, was a Postdoc research scholar at the Institute

of Informatics and Telecommunications at the National Centre for Scientific Research "Demokritos", Athens, Greece. During 2008–14 he was an Assistant Professor in the Department of Informatics & Telecommunications at the University of Peloponnese, in Tripolis, Greece, where currently is an Associate Professor. Between 2014–16 he served as the Head of DIT.

Dr. Sagias research interests span the broad area of digital communications, and more specifically include MIMO and cooperative systems, fading channels, satellite communications and optical-wireless communication systems. In his record, he has over fifty (50) papers in prestigious international journals and more than thirty (30) in the proceedings of world recognized conferences. For five (5) years (between 2009–14) he was an Associate Editor of IEEE Transactions on Wireless Communications, while before 2009 he had served as an Editor for AEÜ - International Journal of Electronics and Communications

and IETE Technical Review. Additionally, he is serving as a reviewer and TPC member for various IEEE conferences (GLOBECOM, ICC, VTC, etc). He is a co-recipient of the best paper award in communications in the IEEE Wireless Communications and Networking Conference (WCNC), Istanbul, Turkey, May 2014 and 3rd International Symposium on Communications, Control and Signal Processing (ISCCSP), Malta, March 2008. He is a senior member of the IEEE and IEEE Communications Society as well as the Hellenic Physicists Association.



Anthony C. Boucouvalas received the B.Sc. degree in Electrical and Electronic Engineering from Newcastle upon Tyne University, Newcastle, U.K., in 1978, the M.Sc. and D.I.C. degrees in Communications Engineering from Imperial College, University of London, London, U.K., in 1979, and the Ph.D. degree in fiber optics from Imperial College, in 1982. Subsequently, he joined the GEC Hirst Research Center and became Group Leader and Divisional Chief Scientist working on fiber-optic components, measurements, and sensors until 1987, when he joined Hewlett Packard Labora-

tories (HP) as a Project Manager. At HP, he worked in the areas of optical communication systems, optical networks, and instrumentation, until 1994, when he joined Bournemouth University, Bournemouth, U.K. In 1996, he became a Professor in Multimedia Communications, and in 1999 he became Director of the Microelectronics and Multimedia research Center. Currently, he is the Head of Department of Telecommunications Science and Technology, University of Peloponnese, Greece. His current research interests span the fields of wireless communications, optical fiber communications and components, multimedia communications, and human-computer interfaces where he has published over 250 papers. He has contributed to the formation of IrDA as an industry standard and he is now a member of the IrDA Architectures Council contributing on new IrDA standards.

Dr. Boucouvalas is a Fellow of the Royal Society for the encouragement of Arts, Manufacturers and Commerce, Fellow of Institute of Electrical Engineers (IEE) and, in 2002, became Fellow of IEEE, for contributions to Optical fiber components and optical wireless communications. He is a Member of the New York Academy of Sciences and ACM. He is an Editor of the IEEE Wireless Communications Magazine, IEEE TRANSACTIONS ON WIRELESS NETWORKS, Associate Editorial Member for the Wireless Communications and Mobile Computing Journal and Vice Chairman of the IEEE UK&RI Communications Chapter. He is in the Organizing Committee of the International Symposium on Communication Systems Networks and Digital Signal Processing, (CSNDSP), and a member of Technical Committees in numerous conferences.